JOURNAL OF MATERIALS SCIENCE 29 (1994) 5219–5231

Review
The toughening and strengthening of ceramic materials through discontinuous reinforcement

KENONG XIA
Department of Mechanical and Manufacturing Engineering, University of Melbourne, Parkville, Victoria 3052, Australia

TERENCE G. LANGDON
Department of Materials Science and Mechanical Engineering, University of Southern California, Los Angeles, CA 90089 1453, USA

The incorporation of a discontinuous reinforcement, in the form of fibres or particulates, into a ceramic matrix provides the possibility of introducing toughness and strength. This review summarizes the various toughening and strengthening mechanisms and then examines and analyses the reported experimental observations on various ceramic composite systems.

1. Introduction

Ceramic materials possess several advantages, such as high strength and hardness, high elastic modulus and excellent resistance to severe thermal and chemical environments. Nevertheless, a major concern in using ceramic materials is their inherent brittleness which has the potential of greatly restricting their reliability in service. Within the last decade the development of ceramic matrix composites has attracted considerable attention and a major effort has developed to improve the toughness of ceramics and thereby to realize their potential applications in service operations. This review provides a brief overview of these developments.

2. The role of residual stresses

A ceramic matrix composite consists of a matrix, which is a ceramic material, and reinforcements, which are usually also ceramics, i.e. two phases are involved. When a second phase is combined into a matrix there is usually a mismatch between them in terms of the structural, mechanical and/or physical properties. Two mismatches pertinent to the toughening and strengthening of ceramics are the differences in thermal expansions and the elastic moduli. In addition, interfaces are introduced into the matrix and the strength of these interfaces plays an important role in dictating the operating toughening mechanisms and the effectiveness of the second phase in contributing to strengthening.

The different thermal contractions shown by the second phase and the matrix phase give rise to residual stresses when the composite is cooled down from the fabrication temperature. If the coefficient of thermal expansion of the reinforcing phase (fibres or particulates) is greater than that of the matrix, the field of residual stresses in the matrix consists of circumferential compression and radial tension and the fibre is in axial tension, as shown in Fig. 1. Conversely, when the coefficient of thermal expansion of the reinforcing phase is less than that of the matrix, circumferential tensile stresses and radial compressive stresses are created in the matrix so that the fibre is then in axial compression, as shown in Fig. 2; for example, such a stress field was detected in the system of an Al_2O_3 matrix with SiC whiskers using neutron diffraction [1]. By choosing an appropriate combination of the second phase and the matrix, the type and the magnitude of the residual stress field may be controlled so that several toughening mechanisms are achieved.

A more limited way of producing stresses in the matrix is through a phase transformation. Some second phases undergo a martensitic transformation which involves volumetric changes when the composite is cooled. This also leads to stresses in the matrix and the process may be utilized to toughen the material. The most prominent example of the latter process is found in zirconia-toughened ceramics (ZTC).

In the following sections, various toughening and strengthening mechanisms are reviewed and they are examined by reference to observations on some ceramic–matrix composites. The scope of this review is specifically limited to discontinuously-reinforced composites. Continuously-reinforced composites may display different behaviour in some cases, although they also incorporate many of the same principles.

3. Toughening mechanisms

3.1. Microcracking

As already noted, a misfit between the coefficients of thermal expansion introduces a stress field in the matrix. Such stresses can produce spontaneous microcracks if the residual stresses are sufficiently large [2]. However, the preferred situation in toughening is to

0022–2461

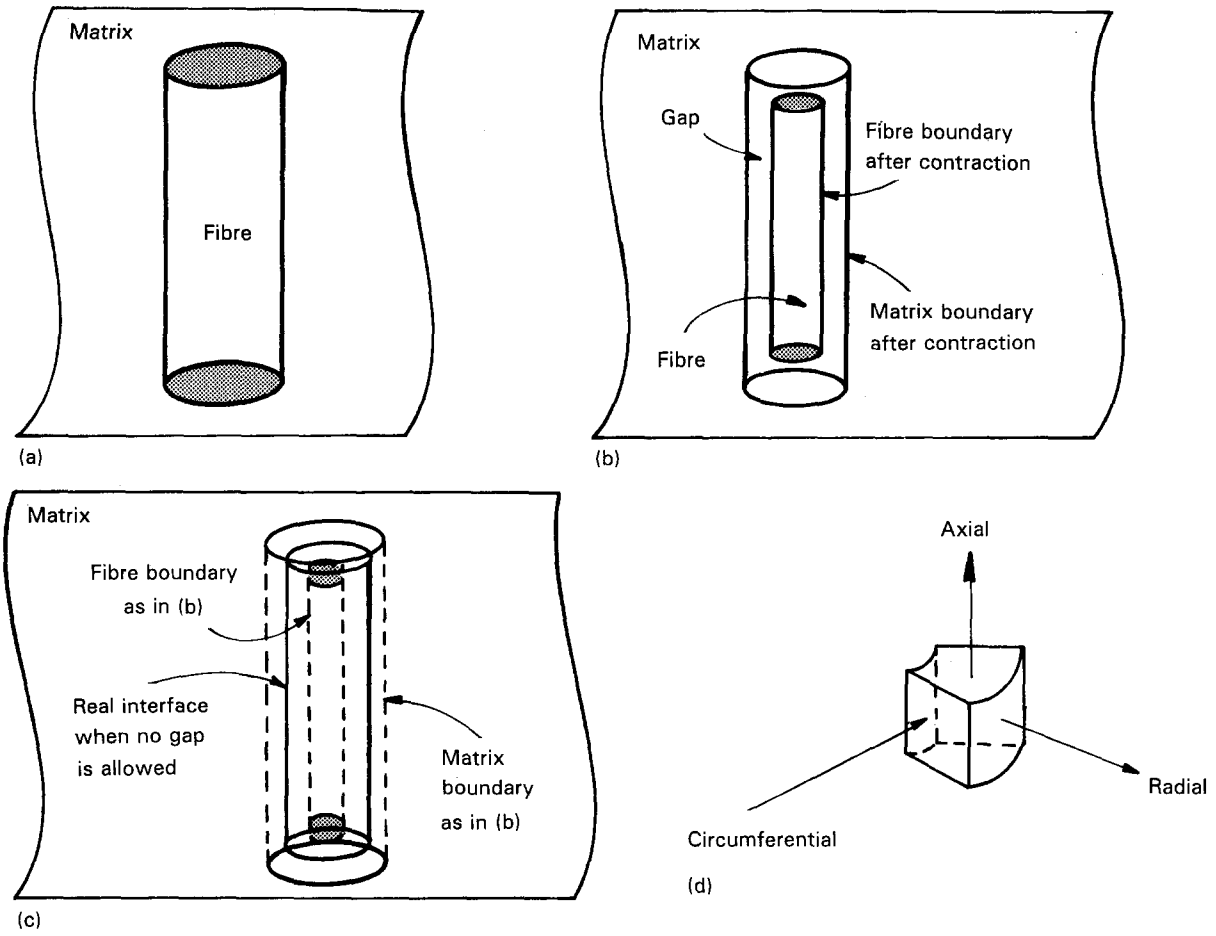

Figure 1 A fibre in a matrix when the thermal expansion coefficient of the fibre is greater than that of the matrix (a) at the fabrication temperature, (b) at room temperature without constraining the fibre and matrix to remain in contact and (c) at room temperature when contact between the fibre and the matrix is retained. (d) Illustrates the stress condition in the fibre in the case of (c).

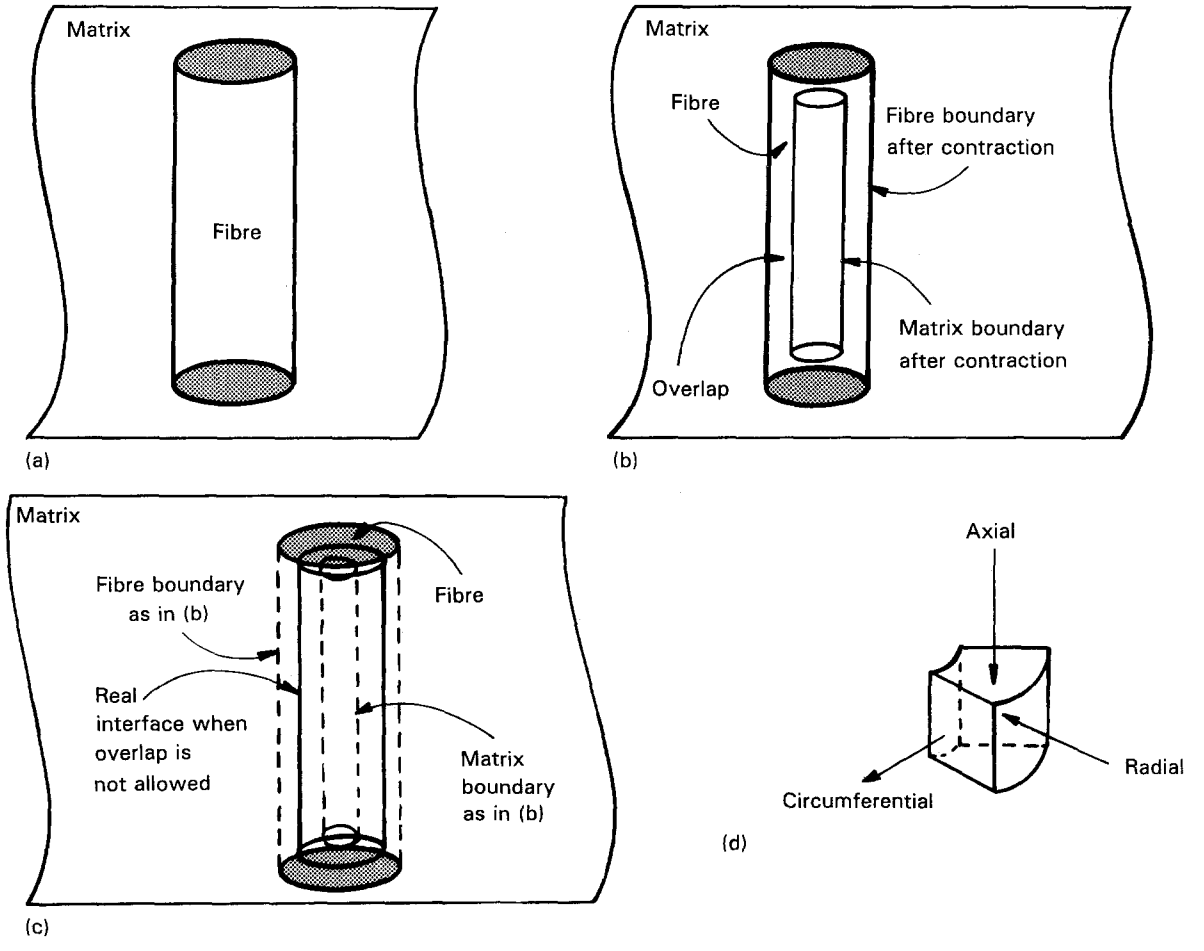

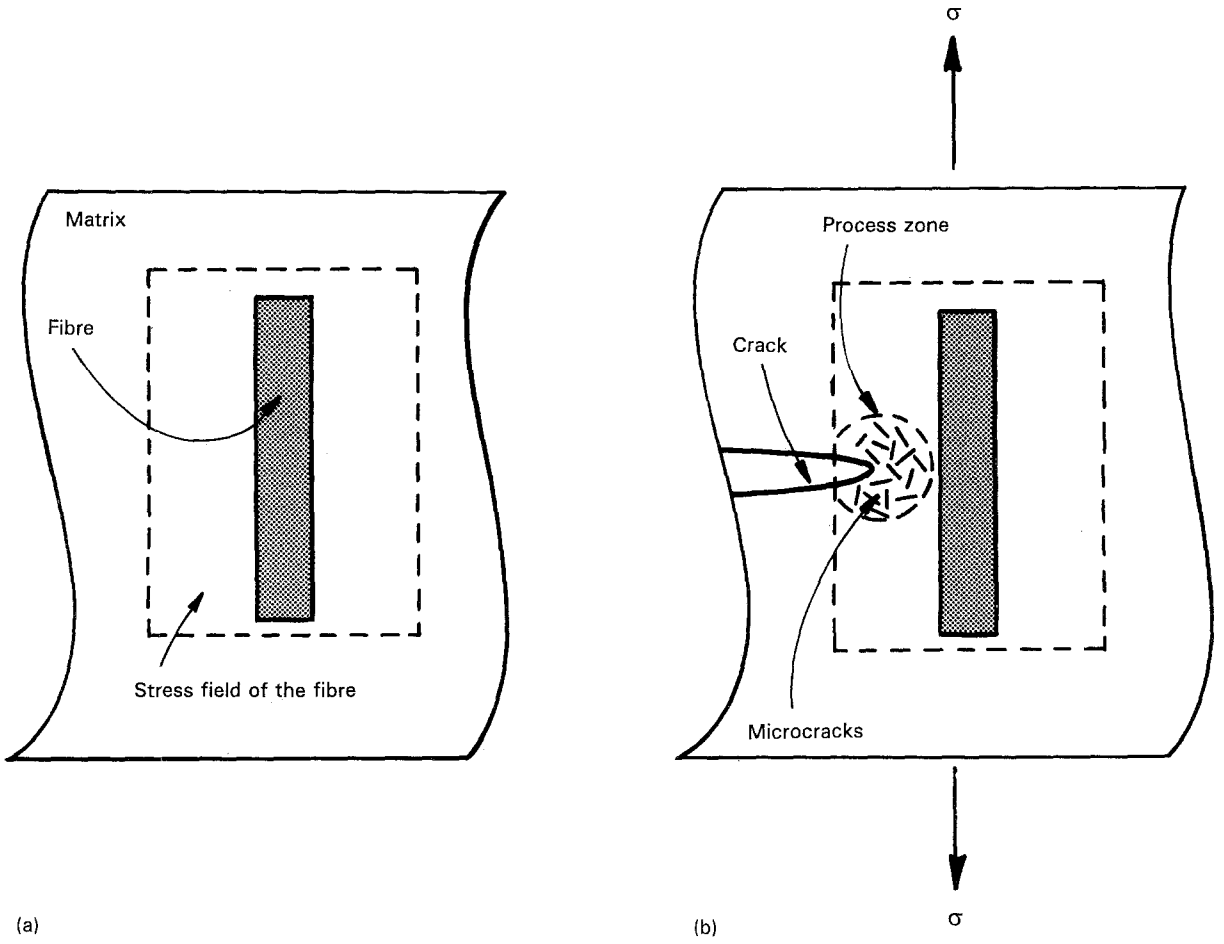

Figure 3 Microcracking toughening mechanism: (a) thermal residual stress field alone and (b) combination of the thermal stresses and the applied stresses causing microcracking in a process zone in front of a macrocrack.

create a stress field that will not produce cracks without the application of a superimposed extrinsic stress field. In this way microcracks are present only at the vicinity of the tip of a macrocrack where a stress concentration is available, thereby forming a process zone [3–5]. Using this procedure the stress intensity at the crack tip is reduced and the toughness is increased. The principle of this mechanism is shown schematically in Fig. 3, where σ is the applied stress.

The energy dissipated in generating microcracks is used primarily to create new surfaces. The increase in fracture energy of the primary crack is expected to be directly proportional to the surface energy of the microcracks, the volume fraction of second-phase particles or fibres producing the microcracks and the size of the process zone [6]. Under a fixed residual stress field there is a critical fibre or particle size above which the fibre or particle will develop spontaneous microcracks [2]. Thus, in order to increase the number of fibres or particles contributing to the toughening, it is necessary to keep the fibres or particles below this critical size. In practice, analysis indicates that maximum toughening necessitates having a narrow distribution of particle sizes close to the critical size [7].

The microcracks thus formed reduce the elastic modulus within the process zone. This serves to lower the near-crack tip stress intensity factor and thus to shield the crack tip from the applied stress field [8]. If not controlled, however, excessive microcracks may also lead to a decrease in fracture toughness [9].

In addition, the main crack may be deflected or it may branch due to the presence of these microcracks, and this provides the potential for additional toughening.

3.2. Crack deflection and branching

The direction of the extension of a crack may change when the crack meets an obstacle such as a second-phase particle or fibre. There are several possible situations, as illustrated schematically in Fig. 4. In practice, this deviation in direction means that the crack travels a longer path and the stress intensity at the crack tip is reduced since the plane of the crack is no longer perpendicular to the tensile stress. In the case of fibre reinforcements, the crack may be deflected to extend along the interface between the fibre and the matrix, as shown in Fig. 4a, and this facilitates

Figure 2 A fibre in a matrix when the thermal expansion coefficient of the fibre is smaller than that of the matrix (a) at the fabrication temperature, (b) at room temperature when the fibre and matrix are hypothetically not constrained to retain a common interface and (c) at room temperature when a common interface between the fibre and the matrix is retained. (d) Illustrates the stress condition in the fibre in the case of (c).

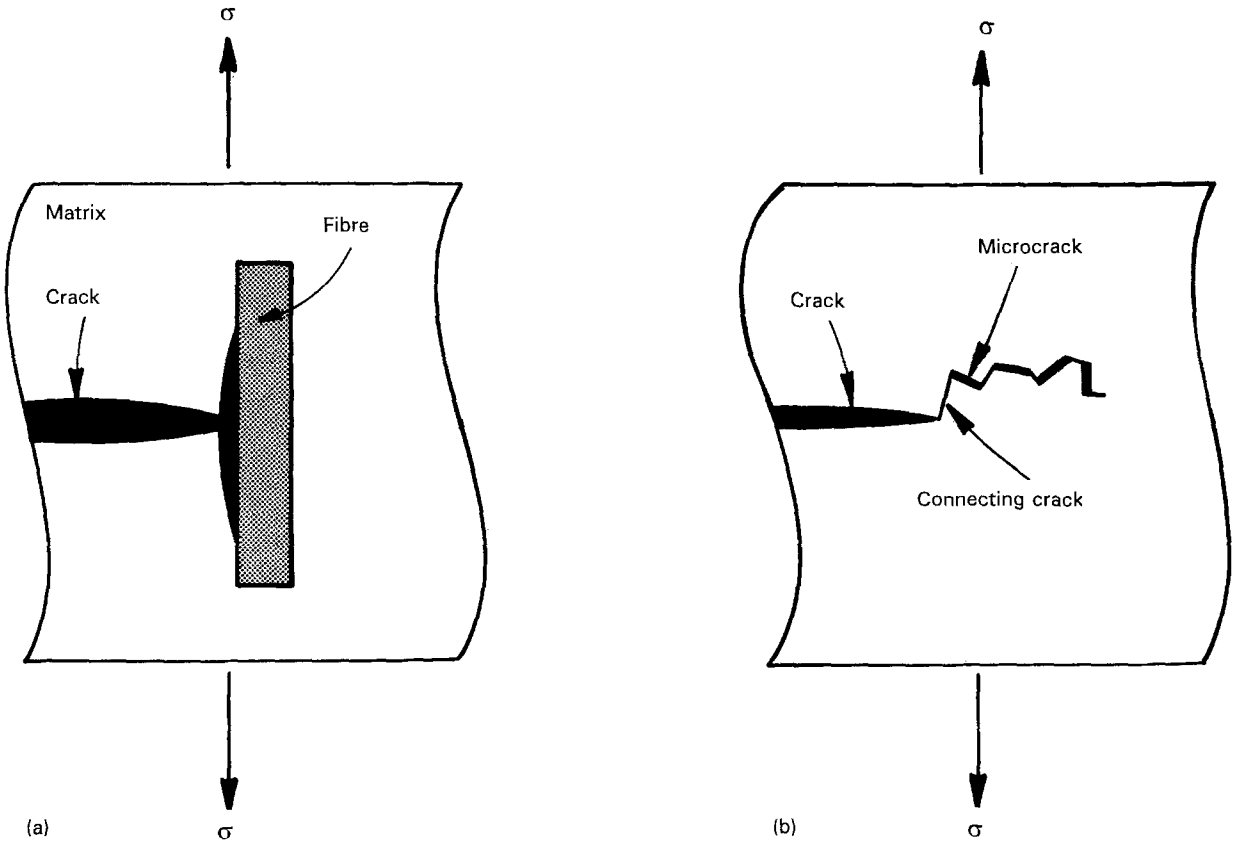

Figure 4 Toughening by crack branching or deflection: (a) a crack deflected along the interface and (b) a crack deflected by connecting to microcracks.

fibre pull-out which is another toughening mechanism (see Section 3.3). The microcracks ahead of the crack tip may also attract the crack and thereby cause it to deflect, as shown in Fig. 4b. Crack branching results when the crack bifurcates into more than one direction.

In general, a crack propagates perpendicular to the tensile axis and parallel to the compressive stress. This means that a residual stress field may also deflect the crack. For example, a particle having a thermal expansion coefficient higher than the matrix has around it a radial tension and a hoop compression. Such a stress field produced by a particle in the plane of a crack may deflect the crack and force it to travel around the particle [10]. In addition to crack deflection, the compressive stress field at a distance from the particles also contributes to enhancing toughness in such a system [11].

The treatment of crack deflection has been developed theoretically [12] and examined experimentally [13]. It is concluded that a rod-shaped second phase with a high aspect ratio is most effective in enhancing toughness. The toughness is also improved by increasing the volume fraction of the second phase, but it is independent of the size of the second phase. The most important contribution to toughening by deflection comes from a twist after an initial tilt of the crack front (i.e. the crack front is deflected off the original plane, followed by its rotation around the axis perpendicular to the fracture plane).

Such a crack-deflection mechanism of toughening was recently modified to include microstructural parameters such as volume fraction, shape, size, orientation and distribution of the second-phase particles [14]. According to this model, the direct contribution to toughening from crack deflection may be less than predicted by the earlier theory [12].

3.3. Fibre pull-out

When a tensile load is applied to a composite, the load is transferred to the reinforcement by shearing along the interface between the fibres and the matrix. A shear stress, τ_s, is established at the interface between the fibre and the matrix, and this shear stress leads to a tensile stress, σ_t, along the axis of the fibre, as shown in Fig. 5.

The relationship between the two stresses is given by [15]

$$\sigma_t = \left(\frac{2l}{d_f}\right)\tau_s \tag{1}$$

where l is the length of the fibre and d_f is the fibre diameter. If σ_t is less than the failure stress of the fibre, σ_f, and τ_s reaches the shear strength of the interface, τ_i, fibre pull-out will take place.

For any selected composite system, the values of σ_f and τ_i are fixed. Therefore, the condition of $\sigma_t < \sigma_f$ when $\tau_s = \tau_i$ is satisfied only if l/d_f is less than $\sigma_f/2\tau_i$. This leads to the definition of a critical aspect ratio for the fibre, given by

$$\left(\frac{l}{d_f}\right)_c = \frac{\sigma_f}{2\tau_i} \tag{2}$$

or, when the diameter of the fibre is fixed, a critical

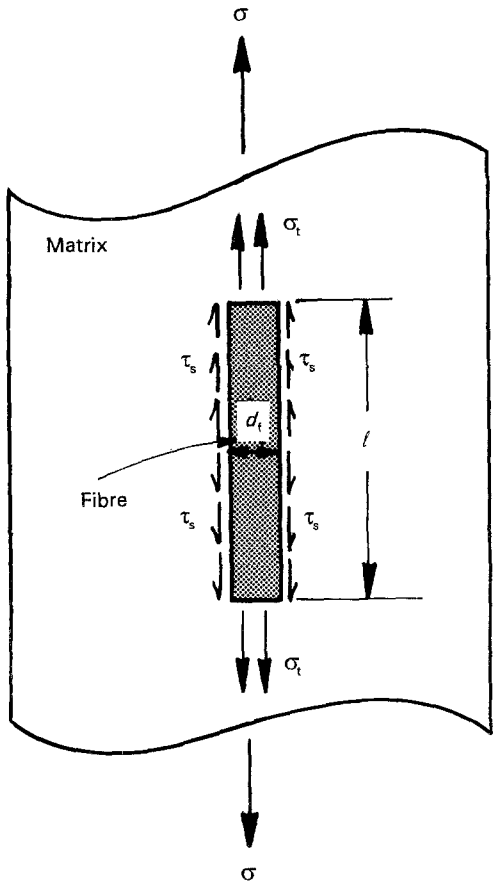

Figure 5 Stresses acting on a fibre due to the matrix under the application of a tensile stress.

length, l_c, given by

$$l_c = \frac{\sigma_f d_f}{2\tau_i} \quad (3)$$

At lengths below this critical value the fibre is pulled out before fracture. At lengths above this critical value the fibre is broken without pull-out.

Fibre pull-out requires additional work and thus toughening effects are achieved in the process. From Equation 3, it is seen that a weaker interface gives a greater critical length for the fibres. Thus, more fibres participate in the pull-out process and hence more toughening is achieved. However, the interface must be sufficiently strong to give a reasonably high work of pull-out and to minimize the possible decrease in strength.

The interfacial shear strength depends on the bond between the matrix and the fibre. The bonding may result from a chemical reaction or mechanical friction, or from a combination of the two. Although the contribution from a chemical reaction is difficult to estimate, it is generally possible to assess the bond strength arising from mechanical factors.

If the normal stress across the interface is σ_n and the friction coefficient of the interface is μ, the shear strength arising from mechanical bonding is given by

$$\tau_i^m = -\mu\sigma_n \quad (4)$$

where $\sigma_n < 0$ (compression); otherwise $\tau_i^m = 0$. The value of σ_n can be obtained from the relationship [16]

$$\sigma_n = \frac{(\alpha_f - \alpha_m)\Delta T}{\frac{1+\nu_m}{2E_m} + \frac{1-2\nu_f}{E_f}} \quad (5)$$

where α denotes the coefficient of thermal expansion, ν is Poisson's ratio, E is Young's modulus and ΔT is the temperature differential between the temperature below which stress relaxation cannot take place and the temperature under consideration: the subscripts m and f refer to the matrix and the fibres, respectively.

It follows from Equation 5 that when $\alpha_f > \alpha_m$ the value of σ_n is positive (tensile stress) and there is no mechanical bonding. Chemical bonding is then necessary for pull-out toughening. On the other hand, if $\alpha_f < \alpha_m$ a mechanical bonding arises with a strength of τ_i^m.

Both mechanical and chemical bonding usually exist in practice, although one of them may be dominant. In addition, the friction coefficient of the interface is dependent upon the chemical reaction between the matrix and the fibres. It is possible to alter the interfacial characteristics by changing the surface conditions of the reinforcement so that the toughening effect from fibre pull-out is increased [17]. Toughening from fibre pull-out can be enhanced also by increasing the length of the fibres [18].

The shear strength of the interface may be determined experimentally for fibre reinforced composites by pushing or pulling fibres to slide in a ceramic matrix [19–22]. Reasonably comprehensive analyses of such processes have been developed [23, 24], taking into consideration the chemical bonding, residual stresses and surface roughness of the fibres [23].

3.4. Crack bridging

In the crack bridging mechanism, shown schematically in Fig. 6, the front of a crack passes beyond the reinforcing fibres but the fibres remain intact and bridge the fracture surfaces in the wake of the crack. The open displacement of the crack is then limited and this makes further propagation of the crack difficult.

Several theoretical analyses of the bridging process have been proposed [25–28]. The toughness of the composite is improved by increasing the strength, the diameter and the volume fraction of the reinforcements. An important factor is to prevent damage to the fibres by passage of the crack. This requires either partial debonding of the fibres from the matrix at the crack tip or a high strength for the fibres. Contributions from bridging by large matrix grains have also been reported [29].

Experimental evidence for crack bridging [27, 30] indicates that debonding of the fibres occurs along the interfaces. Whisker bridging has also been observed *in situ* [31].

3.5. Crack pinning

Unlike crack bridging, where a crack tip passes beyond a reinforcement fibre, crack propagation may be stopped and the crack pinned at the fibres or particles.

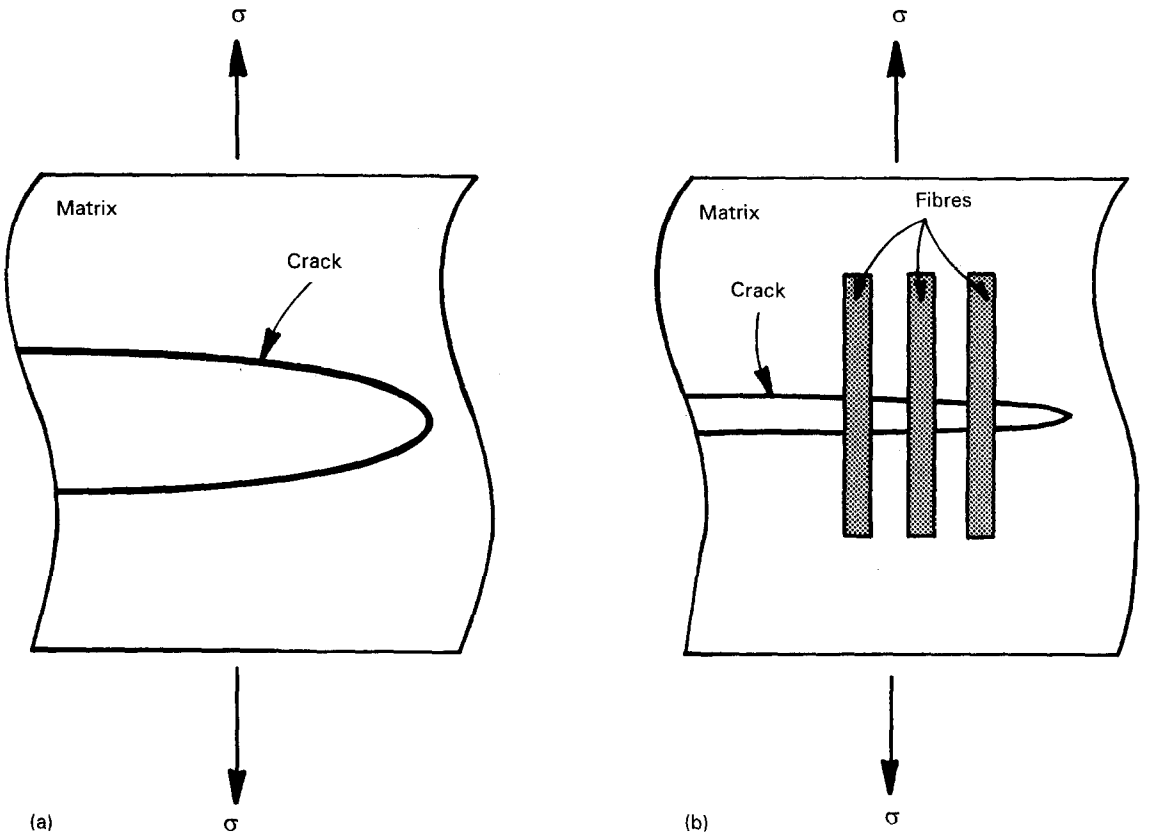

Figure 6 Toughening by crack bridging: (a) a crack in a matrix with no fibres and (b) a crack bridged by fibres.

A model has been developed where the increase in fracture energy is attributed to the bowing out of the crack front between the fibres or particles, as illustrated in Fig. 7 [32]. It is clear that such a mechanism demands both a strong reinforcement and a good interface so that the fibres or particles can act as barriers. Also, the spacing between the reinforcements must be small compared to the crack size in order for this mechanism to be effective.

3.6. Phase transformation

The use of a phase transformation is a novel and attractive mechanism of toughening, but it is limited to materials containing a phase that undergoes a transformation during the fracture process. This transformation is usually martensitic, so that it involves a change in the volume and/or shape of the second-phase particles, and it is diffusionless and athermal.

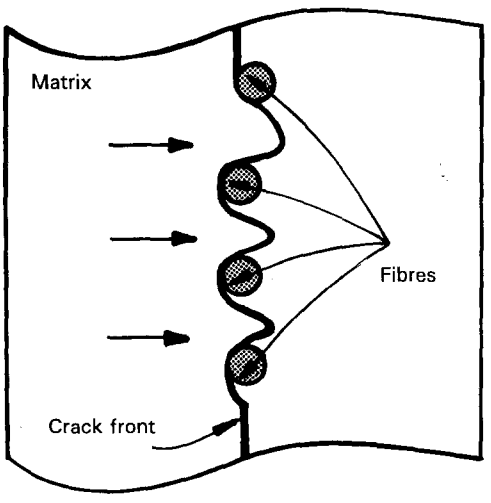

Figure 7 A crack front pinned by fibres.

If such a phase is unconstrained, it will transform from its present metastable structure at high temperatures to a stable structure at low temperatures when the temperature is decreased. However, the strain energy associated with the shape change during transformation may prevent the process from occurring when the phase particles are contained in a stable matrix. For the transformation to take place, an appropriate stress field is necessary to provide this energy. As a result, the stress field is reduced.

Toughening takes place when a crack propagates through a matrix containing such phases, since the stress field of the crack tip is relieved by the transformation of the second-phase particles near the crack. A transformation zone is formed in front of the crack tip within which the stress intensity is greatly decreased, and further propagation of the crack then requires an increase in the level of the applied stresses. Many theories have been developed to analyse the toughening behaviour through phase transformations [33–36] and the various transformation–toughening mechanisms have been reviewed [37].

To date, most attention has focused on the use of a phase transformation in the toughening of zirconia. This material has a tetragonal structure at high temperatures and a monoclinic symmetry at low temperatures. The temperature for the start of the transformation when cooling zirconia is $\sim 1125\,K$ [38]. The transformation gives rise to an increase in volume

of $\sim 4\%$ and a shear distortion of $\sim 7\%$ [39]. It is possible to calculate the stresses and strain energy brought about by the transformation and to analyse the transformation conditions [40]. Optimum toughening is achieved by having most particles very close to the transformation conditions in the absence of external stresses so that a larger transformation zone is available (e.g. having particles that are just smaller than the critical size above which spontaneous transformation will occur without the additional stress field [6]).

The microstructures of ZTC have been analysed in some detail [41]. The three most fundamental microstructures are: (1) partially-stabilized zirconia (PSZ) with large cubic matrix grains and dispersed coherent precipitates of tetragonal structure; (2) tetragonal zirconia polycrystals (TZP) with fine grains; and (3) a ceramic matrix with dispersed tetragonal zirconia particles. With careful control, these microstructures can lead to a significant improvement in the fracture strength and toughness of ceramic materials [42, 43].

In practice, zirconia toughening is complex and may include transformation toughening, microcracking toughening and deflection toughening [44, 45]. Some investigations have shown that microcracking is a more important toughening mechanism in zirconia-toughened alumina [46, 47]. Since the effects from a phase transformation and microcracking decrease in importance with increasing temperature, crack deflection may become of increasing importance at elevated temperatures. Several methods have been proposed to increase the toughness at high temperatures in ZTC, including a combination of transformation toughening at low temperatures and fibre reinforcement at the higher temperatures [38].

Finally, when zirconia is incorporated to improve other matrices, the toughening is most effective when the matrices have a yield strength of $\geqslant 450$ MPa, a close match in elastic modulus with zirconia and strong interfaces with zirconia particles [48].

3.7. Summary

Having reviewed the toughening mechanisms, it should be noted that more than one mechanism usually operates simultaneously in any composite [49, 50]. Several individual mechanisms may interact with each other; for example, microcracking and crack bridging may precede pull-out, and crack deflection may be attracted by the microcracks. The focus of much current research is to identify the various possible toughening mechanisms in a particular composite and then to effectively combine these mechanisms to produce a tough composite.

4. Strengthening mechanisms

4.1. Load transfer

The difference between the value of Young's modulus for the fibres and the matrix gives rise to different stresses in the fibres and in the matrix when they are deformed to the same strain. If the Young's modulus of the fibres is much greater than that of the matrix, then the fibres carry more load than the matrix. Therefore, this requires good interfaces that remain sufficiently strong to transfer the load from the matrix to the fibres. For whisker reinforced composites it is often desirable to increase the length of the whiskers [18]. In addition, it is usually required that the ratio of Young's modulus of the fibres to that of the matrix is greater than two to achieve a significant increase in strength [51]. This is often not the case in ceramic matrix composites where toughening instead of strengthening is the main concern.

4.2. Pre-stressing of the matrix

If the coefficient of thermal expansion of the fibres is greater than that of the matrix, compressive stresses develop in the matrix when the composite is cooled down from the processing temperature. Under these conditions the external tensile stresses will be reduced by superimposition of such a compression field.

4.3. Strengthening through toughening

The fracture strength, σ_f, of a material is related to its fracture toughness, as measured by the critical stress intensity factor, K_{IC}, through the relationship

$$\sigma_f = \beta\left(\frac{K_{IC}}{c^{1/2}}\right) \tag{6}$$

where c is the critical crack length above which a crack will propagate rapidly to cause failure and β is a constant. Therefore, an increase in K_{IC} may bring about a higher value of σ_f. However, toughening itself may affect the strength of the material. For example, microcracking toughening may decrease the strength when the microcracks are not limited to a small process zone in front of the crack tip or when many spontaneous microcracks develop in the matrix. Since strengthening is a second priority to toughening in ceramic matrix composites, the objective is to achieve a significant improvement in toughness while at the same time maintaining the strength at essentially the same level.

5. Experimental observations on composite systems

Experimentally observed toughening and strengthening effects and mechanisms are now summarized for a number of different ceramic matrix composites. For composites utilizing transformation toughening, PSZ and TZP are not included. The results are presented in Table I. Inspection shows that the toughness in terms of K_{IC} of the matrix material is generally significantly increased, whereas the strength increase is usually only moderate.

The following sections analyse some typical composite systems.

5.1. Al_2O_3 matrix composites

The Al_2O_3 matrix composites tend to be the most thoroughly investigated. The toughness and strength

of the matricies and the composites listed in Table I are plotted schematically in Fig. 8: the spread in values is a consequence of the different processing methods, the materials, the evaluation methods and the nature of brittleness in the materials. However, it is apparent that a fracture toughness of $\geqslant 10\ MPa\ m^{1/2}$ and a flexural strength of > 600 MPa may be achieved in these composites. SiC whiskers and ZrO_2 particles are the most common reinforcements, and it appears that ZrO_2 is slightly more effective.

5.1.1. Al_2O_3 with SiC whiskers

The tensile strength and the Young's modulus at room temperature of SiC whiskers is reported to be ~ 7 and ~ 700 GPa, respectively [51, 55]. The shear modulus of the Al_2O_3 matrix may be estimated from the

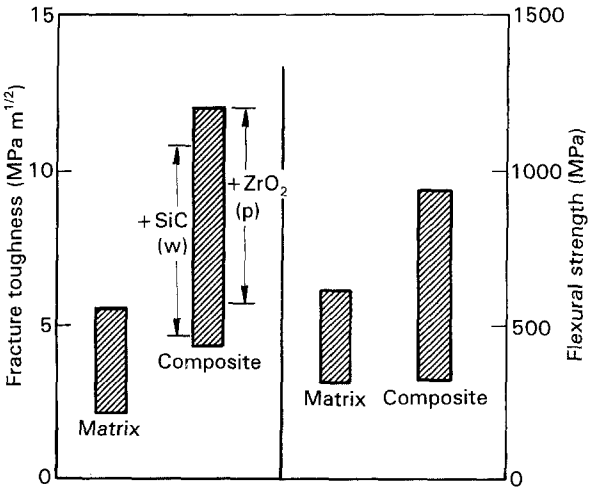

Figure 8 Fracture toughness and flexural strength of Al_2O_3 matrix and Al_2O_3 matrix composites (p, particles; w, whiskers).

TABLE I Summary of strengthening and toughening effects in ceramic composites

Material[a] (matrix + reinforcement)	K_{IC} (MPa m$^{1/2}$)			Flexural strength (MPa)			Major toughening mechanisms	Ref.
	Matrix	Composite	Increase (%)	Matrix	Composite	Increase (%)		
Al_2O_3 + 15 vol % B_4C (w)	~ 4.0	~ 7.5	88	~ 400	~ 500	25	–	[52]
Al_2O_3 + 5 vol % B_4C (p)	~ 4.0	~ 5.5	38	~ 400	~ 600	50	–	[52]
Al_2O_3 + 30 wt % Sialon	3.5	4.3	23	–	–	–	–	[53]
Al_2O_3 + 30 vol % SiC (w)	5.0	9.5	90	385	650	69	Whisker pull-out; crack deflection and bridging	[51]
Al_2O_3 + 20 vol % SiC (w)	4.6	8.7	89	600	800	33	Whisker pull-out; crack deflection	[54, 55]
Al_2O_3 + 15 vol % SiC (w)	–	7.0	–	–	330	–	–	[56]
Al_2O_3 + 30 vol % SiC (w)	2.1	4.6	119	–	652	–	–	[57]
Al_2O_3 + 40 wt % SiC (w)	~ 4.0	~ 8.0	100	~ 480	~ 700	46	–	[58]
Al_2O_3 + 30 vol % SiC (w)	–	6.0–8.7	–	–	–	–	Whisker pull-out; crack deflection	[17]
Al_2O_3 + 33 vol % SiC (w)	–	7.6–9.8	–	–	–	–	Microcracking	[9]
Al_2O_3 + 25 vol % SiC (w)	~ 3.0	~ 10.7	257	~550–600	~ 550–600	0	Whisker pull-out/bridging; crack deflection	[59]
Al_2O_3 + 5 vol % SiC (p)	3.0	4.5	50	–	–	–	Microcracking	[60]
Al_2O_3 + 30 vol % SiC (p)	4.3	~ 7.0	63	610	480	– 21	–	[61]
Al_2O_3 + 5 vol % TiB_2 (p)	~ 4.0	~ 6.5	63	~ 420	~ 650–700	55–67	–	[62]
Al_2O_3 + 15 vol % ZrO_2	–	10.0	–	–	–	–	Microcracking	[63]
Al_2O_3 + 15 vol % ZrO_2	~ 5.5	~ 9.0	64	~320–480	~ 480–940	–	–	[64]
Al_2O_3 + 5–8 vol % ZrO_2	~ 5.0	~ 8.0	60	~ 450	~ 600	33	–	[65]
Al_2O_3 + 20 vol % ZrO_2	4.7	8.7	85	–	–	–	Transformation; microcracking	[66]
Al_2O_3 + 15 vol % ZrO_2	~3.5–4.0	~ 5.7–6.0	–	–	–	–	Transformation; microcracking	[67]
Al_2O_3 + 12 vol % ZrO_2 (single crystals) + 40 vol % TZP	–	~ 12.0	–	–	–	–	Transformation; microcracking; crack deflection	[68]
Mullite + 30 wt % SiC (w)	2.5	3.5	40	180	386	114	–	[69]
Mullite + 30 wt % SiC (w)	~ 2.3	~ 4.7	104	~ 350 400	~ 500	25–43	–	[70]
Mullite + 35 wt % Y–ZrO_2	~ 2.3	~ 4.0	74	400	~ 400–450	–	–	[70]
Mullite + 30 wt % SiC (w) + 35 wt % Y–ZrO_2	~ 2.3	~ 6.2	170	400	~ 700	75–100	–	[70]
Mullite + 10 vol % SiC (w)	1.8	~ 2.5	39	191	~ 255	34	Whisker pull-out; whisker/matrix interaction	[71]
Mullite + 10 vol % SiC (p)	1.8	~ 2.4	33	191	~ 260	36	–	[71]
Mullite + ZrO_2 (p)	2.0	3.0	50	–	–	–	Grain boundary strengthening	[72]
Mullite + 15 vol % ZrO_2 (p)	2.0	~ 3.1	55	–	–	–	–	[73]
Mullite + 20 vol % SiC (w)	2.0	~ 4.7	135	–	–	–	–	[73]
Mullite + 20 vol % ZrO_2 (p) + 20 vol % SiC (w)	2.0	7.0	250	–	–	–	–	[73]

TABLE I Continued.

Material[a] (matrix + reinforcement)	K_{IC} (MPa m$^{1/2}$)			Flexural strength (MPa)			Major toughening mechanisms	Ref.
	Matrix	Composite	Increase (%)	Matrix	Composite	Increase (%)		
Sialon + 10 vol % Y–ZrO_2	3.1	5.5	77	–	–	–	Transformation	[74]
Sialon + 20 vol % Y–ZrO_2	3.1	6	94	–	–	–	Transformation	[74]
Sialon + 30 vol % Y–ZrO_2	3.1	7.5	142	–	–	–	Transformation	[74]
SiC + 10 wt % AlN	2.8	4.7	68	–	–	–	–	[75]
SiC + TiB_2 (p)	4.6	8.0	74	–	–	–	Crack deflection	[76]
SiC + 25 vol % TiC (p)	4.0	6.0	50	500	> 700	> 40	Crack deflection	[10]
SiC + 40 vol % TiC (p)	~ 1.8	~ 6.0	233	–	–	–	Crack deflection	[77]
Si_3N_4 + 30 vol % SiC (w)	4.5	6.4	42	750	950	27	Crack deflection; whisker pull-out	[78]
Si_3N_4 + 20 vol % SiC (w)	~ 3.0	~ 4.2	40	~ 500	~ 500	0	–	[79]
Si_3N_4 + 20 vol % SiC (w)	~ 5.0	~ 7.5	50	~ 700	⩽ 600	–	Whisker pull-out	[80]
Si_3N_4 + 20 vol % SiC (p)	~ 5.0	~ 8.5	70	~ 700	⩾ 400	–	Crack deflection/branching	[80]
Si_3N_4 + 20 vol % SiC (w) + 20 vol % SiC (p)	~ 5.0	~ 10	100	~ 700	~ 400–500	–	Whisker pull-out; crack deflection/branching	[80]
Si_3N_4 + 20 wt % SiC (w)	7.5	10.2	36	–	1300	–	Crack bridging	[81]
Si_3N_4 + 30 vol % Si_3N_4 (w)	4.0	~ 8.0	100	650	~ 650	0	Whisker bridging and pull-out	[82]
Si_3N_4 + 20 vol % TiC (p)	4.7	7.0	49	–	–	–	Crack pinning; microcracking	[83]
Si_2N_2O + 30 vol % SiC (w)	~ 3	~ 6	100	~ 400	~ 750	88	Crack bridging	[84]
TiB_2 + 30 vol % SiC (w)	~ 5.0	~ 7.0	40	~ 450	~ 550	22	–	[85]
TiB_2 + 15–45 vol % ZrO_2	~ 5.5	6.5–9.5	18–73	–	–	–	Transformation	[86]
TiC + 10 vol % SiC (w)	~ 4.0	~ 6.0	50	~ 550	~ 700	27	–	[85]

[a] w, whisker (fibre); p, particulate.

expression

$$G = G_0 - (\partial G/\partial T)\,T \quad (7)$$

where G_0 is the extrapolated shear modulus at absolute zero (1.71×10^5 MPa [87]) and $\partial G/\partial T$ is the variation in G K^{-1} (23.4 MPa K^{-1} [87]). Thus, G is ~ 164 GPa at $T = 298$ K (room temperature). The value of Young's modulus, E, is then obtained from

$$E = 2G(1 + \nu) \quad (8)$$

where ν is Poisson's ratio. For alumina, $\nu \approx 0.3$ and $E \approx 426$ GPa at room temperature. The ratio of the elastic modulus of the SiC whiskers, E_w, to that of the Al_2O_3 matrix, E_m, is ~ 1.6. Thus, strengthening through load transfer should not be significant and the limited increase in strength of the composites is attributed to the toughening.

The thermal expansion coefficient for SiC whiskers is ~ $4.7–4.8 \times 10^{-6}$ K^{-1}, whereas that of the Al_2O_3 matrix is $8.8–8.9 \times 10^{-6}$ K^{-1} [51, 55]. Thus, $\alpha_f < \alpha_m$, and a stress field of radial compression and circumferential tension is established in the matrix. The whisker is therefore in axial compression, as illustrated in Fig. 2.

A calculation of the interfacial normal stress may be performed using Equation 5. A normal (compressive) stress of 1600 MPa was estimated at 295 K and the interfacial shear strength was subsequently calculated as 800 MPa from Equation 4 [88]. Such a strong interface may make whisker pull-out difficult at room temperature. In fact, the critical length, l_c, may be derived from Equation 3. Taking $\sigma_f = 7$ GPa, $d_f = 0.6$ μm and $\tau_i = 800$ MPa, l_c is estimated as ~ 2.6 μm [51]. Thus, only those whiskers whose ends are within $l_c/2$ (~ 1.3 μm) from the fracture plane may possibly pull-out. However, when the temperature is raised to 1373 K, σ_n drops to ~ 500 MPa [89] and τ_i to ≈ 250 MPa, so that the critical length is now $l_c \approx 8.4$ μm. Therefore, it is expected that more whisker pull-outs will take place at higher temperatures. This is consistent with experimental observations of whisker pull-outs in the creep fracture of Al_2O_3 composites tested at 1773 K with 18 and 30 vol % SiC whiskers [89].

Most of the investigations on toughening effects in the composites were conducted at room temperature, although it is important to also understand the toughening behaviour at elevated temperatures since many materials will ultimately be used in a thermal environment. With increasing temperature the residual stress field arising from the thermal mismatch is relieved and the interfacial compressive stress is reduced. In addition, the interfacial chemistry may be changed. All of these factors will influence the interaction between the cracks and the whiskers.

The temperature dependence of the toughening mechanisms has been examined experimentally [90]. The interfacial compression stress was shown to decrease from > 1500 MPa at room temperature, to ~ 500 MPa at 1373 K. Nevertheless, this reduced stress was sufficiently large to prevent substantial whisker pull-out. Thus, the fracture surfaces looked similar for samples tested both at room and higher temperatures. The whiskers perpendicular to the fracture surfaces tended to bridge the cracks, while those parallel to the fracture planes deflected the cracks. In

fact, the toughness of the alumina matrix composite suffered only a slight decrease up to $\sim$ 1273 K.

Another important property in the applications of ceramics at high temperatures is their resistance to thermal shock. When the temperature varies with time in a constrained component, or when the temperature is not uniformly distributed, internal stresses develop and may cause damage in the material. Consequently, the overall mechanical properties may be degraded. It has been demonstrated that the addition of SiC whiskers in alumina enhances the thermal shock resistance of the matrix [91]. Quenching a sample of Al_2O_3–20 vol% SiC(w) to give a temperature difference of 900 K resulted in no loss in flexural strength, although repeated quenches led to a minor decrease in strength which may be attributed to fatigue effects. By comparison, pure alumina suffered a significant strength loss when undergoing a temperature difference of $>$ 400 K. The improvement in the composite was attributed to the higher toughness.

Careful examination by transmission electron microscopy has been conducted on samples containing cracks in order to identify the toughening mechanisms in a SiC whisker-reinforced alumina [30]. It was concluded that crack bridging by the whiskers behind the crack tip is the major toughening mechanism. Debonding of some whiskers from the matrix near the fracture surfaces was necessary to keep the whiskers intact although whisker fracture also occurred.

This crack bridging process was further confirmed from mechanical testing where the load was recorded as the crack propagated [92]. It was found that the load versus displacement curve exhibited a sawtooth shape, as shown in Fig. 9. The applied load dropped when crack growth started, but crack propagation was immediately arrested as the load increase was resumed. Therefore, the extension of a crack proceeded in an irregular manner by repeated initiation and arrest, thereby achieving a toughening effect. In this material the arrest of the crack was attributed to crack bridging by the whiskers.

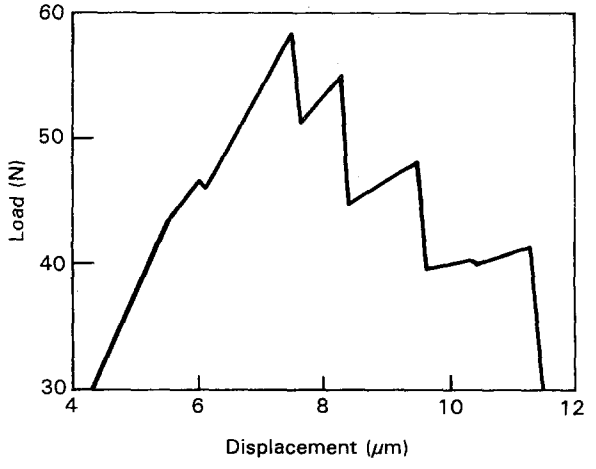

Figure 9 Upper portion of a load versus displacement curve for a SiC whisker-reinforced Al_2O_3 matrix composite, showing the sawtooth shape arising from the crack bridging process [92].

5.1.2. Al_2O_3 with ZrO_2 particles

Both microcracking and transformation toughening take place when the spontaneously-transformed monoclinic. ZrO_2 phase and the metastable tetragonal ZrO_2 phase exist simultaneously in the matrix [93]. Thus, this is a desirable microstructure if an appropriate size distribution of ZrO_2 particles can be achieved (i.e. if tetragonal ZrO_2 particles are transformable and monoclinic ZrO_2 particles can introduce microcracking at the front of a propagating crack). Microcracking toughening in Al_2O_3–ZrO_2 has been investigated experimentally and analysed theoretically for its importance in ZTCs [94].

In addition to improved resistance to catastrophic crack extension in zirconia-toughened alumina, the composite also shows greater resistance to slow crack growth [95]. This was attributed to crack-tip shielding by the transformation zone surrounding the crack. In combination with SiC whiskers, zirconia-toughened alumina shows excellent thermal shock resistance [96].

Large TZP agglomerates, having a size of $\sim$ 20–50 μm, were combined into the alumina matrix in one investigation [68]. Since the tetragonal structure could be retained and the size of the agglomerates was large, the toughening achieved in this composite arose from transformation toughening and crack deflection. Because of the simultaneous presence of TZP dispersoids and single crystal ZrO_2 particles of tetragonal and monoclinic form, multiple toughening effects were obtained from the concurrent operation of the phase transformation, microcracking and crack deflection mechanisms. A fracture toughness of $\sim$ 12 MPa $m^{1/2}$ was achieved in this study.

5.2. Mullite matrix composites

The toughening and strengthening of mullite-based composites are illustrated schematically in Fig. 10, using the data in Table I. It is apparent that a significant increase in both toughness and strength may be achieved.

Studies have been conducted on the toughening effects when both ZrO_2 particles and SiC whiskers are incorporated into the mullite matrix [73]. The results show that the combined toughening effects are equal to or greater than the sum of the individual toughening effects when either toughening method acts alone,

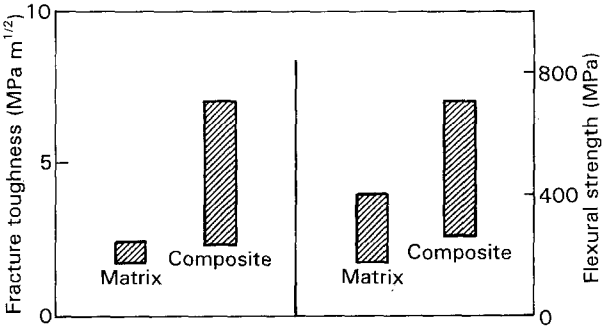

Figure 10 Fracture toughness and flexural strength of mullite and mullite matrix composites.

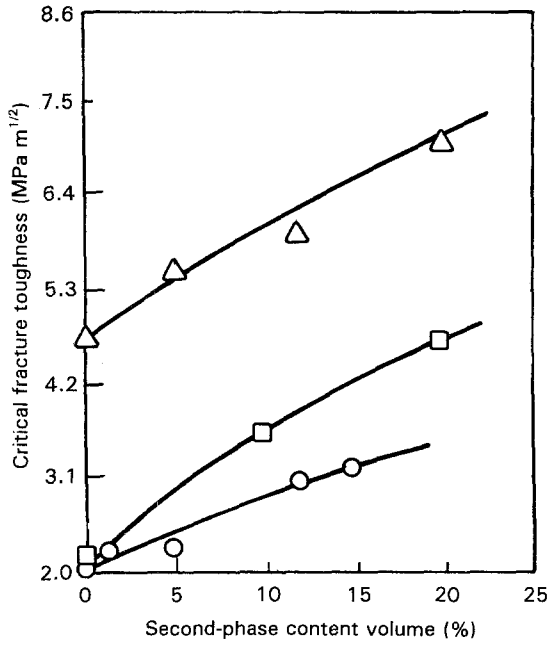

Figure 11 Fracture toughness as a function of second-phase content for three mullite matrix composites [73]. △, Mullite–20 vol % SiC whiskers with ZrO_2 particle additions; □, mullite with SiC whisker additions; ○, mullite with ZrO_2 particle additions.

as indicated in Table I and documented in Fig. 11. It is thus advantageous to combine multiple toughening mechanisms for maximum effect.

5.3. SiC matrix composites

Significant toughening is achieved in SiC matrix composites, as documented in Table I and illustrated schematically in Fig. 12. The coefficients of thermal expansion for TiB_2 and TiC are both greater than for SiC. A stress field of radial tension and circumferential compression is therefore established around these particles. Consequently, crack deflection is the dominant toughening mechanism in these systems because a crack tends to travel perpendicular to the tensile axis and parallel to the compressive stress [10, 76, 77]

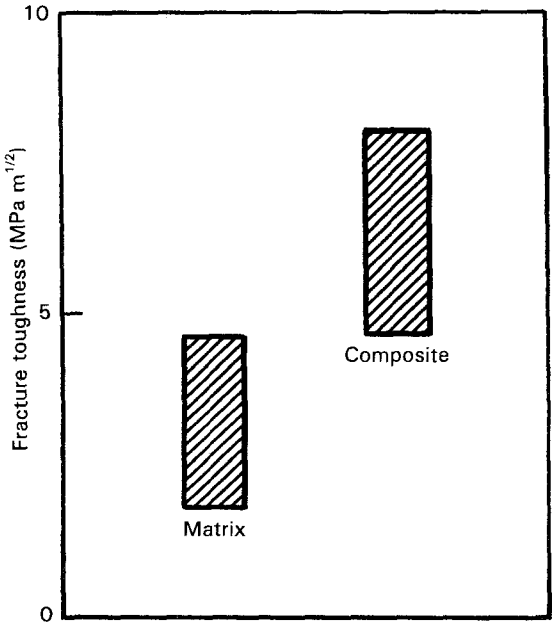

Figure 12 Fracture toughness of SiC matrix and SiC matrix composites.

5.4. Si_3N_4 matrix composites

Although there is an increase in toughness in Si_3N_4 matrix composites, as shown in Table I and depicted schematically in Fig. 13, the strengthening is not significant and indeed the strength of the composites is in some cases lower than in the matrix material.

5.4.1. Si_3N_4 with SiC whiskers or particles

Whiskers are the most common form of reinforcement in the Si_3N_4 matrix. Toughening is generally attributed to crack deflection and microcracking in the matrix [97, 98]. Whisker pull-out is seldom observed, thereby indicating a strong interface. Since Si_3N_4 has a lower thermal expansion coefficient, a tensile normal stress is expected in the interface so that the strong interfacial bonding is probably due to a chemical bonding between the matrix and the whiskers. It appears that a weaker interface may further improve the toughness.

The strength and toughness improvement was also found at high temperatures, up to 1473 K [78]. The toughening mechanisms at all testing temperatures were identified as crack deflection and whisker pull-out. In addition, SiC particulates were added to the Si_3N_4 matrix. It was found that there was a minimum size requirement (about equal to the grain size of the matrix) for the particles to be effective in deflecting cracks and hence toughening the matrix [78].

5.4.2. Si_3N_4 with TiC particles

A wide range of combinations, from 0 to 100 vol % TiC, have been tested for this system [83]. The composites were fabricated by mixing Si_3N_4 and TiC powders, milling and hot-pressing the mixture. A maximum toughness of $\sim 7\ MPa\ m^{1/2}$ occurred with a content of 20 vol % TiC particles. The strength of the Si_3N_4 matrix decreased continuously to that of TiC at

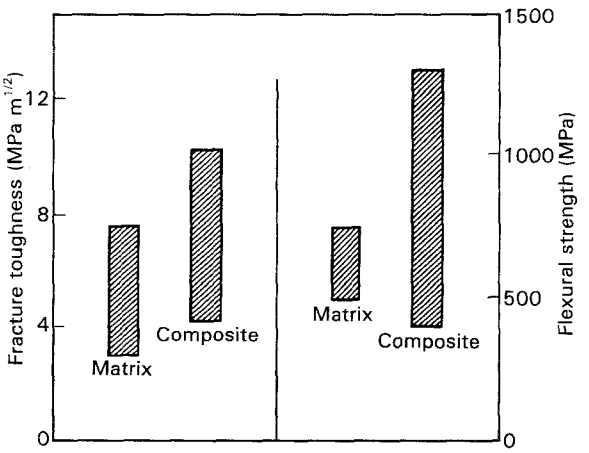

Figure 13 Fracture toughness and flexural strength of Si_3N_4 matrix and Si_3N_4 matrix composites.

~ 50 vol % TiC loading. The initial increase in toughness due to adding TiC particles was attributed to the pinning of the crack front by the particles and to microcracking due to the thermal mismatch. The subsequent decrease in toughness at higher contents of TiC particles was attributed to the overall lower toughness of the particles

6. Summary and conclusions

1. There are various toughening mechanisms that may occur in ceramic composites, including microcracking, crack deflection and branching, fibre pullout, crack bridging, crack pinning and phase transformation. Some of these mechanisms are related processes and in practice several toughening mechanisms may operate simultaneously.

2. For the ceramic composites under consideration in this report, the matrices typically have fracture toughnesses of < 5 MPa $m^{1/2}$ but the composite materials may, under optimum conditions, have fracture toughnesses within the range of ~ 8–12 MPa $m^{1/2}$.

3. Currently, insufficient information is generally available to positively identify the operating, and especially the dominant, toughening mechanisms in any selected composite system.

4. The strengthening of ceramic composites may be achieved through load transfer, pre-stressing and toughening. These effects are not significant in many ceramic systems although the increase in strength in weak matrices may be as large as ~ 100%. Nevertheless, strengthening may be effective at elevated temperatures.

Acknowledgement

This work was supported in part by the US Army Research Office under Grant No. DAAL03-91-G-0230.

References

1. S. MAJUMDAR, D. KUPPERMAN and J. SINGH, *J. Amer. Ceram. Soc.* **71** (1988) 858.
2. R. W. DAVIDGE and T. J. GREEN, *J. Mater. Sci.* **3** (1968) 629.
3. A. G. EVANS, *Scripta Metall.* **10** (1976) 93.
4. *Idem, Acta Metall.* **26** (1978) 1845.
5. D. R. CLARKE, *ibid.* **28** (1980) 913.
6. R. W. RICE, *Ceram. Engng. Sci. Proc.* **2** (1981) 661.
7. A. G. EVANS and K. T. FABER, *J. Amer. Ceram. Soc.* **64** (1981) 394.
8. J. W. HUTCHINSON, *Acta Metall.* **35** (1987) 1605.
9. L. X. HAN, R. WARREN and S. SURESH, *Acta Metall. Mater.* **40** (1992) 259.
10. G. C. WEI and P.F. BECHER, *J. Amer. Ceram. Soc.* **67** (1984) 571.
11. M. TAYA, S. HAYASHI, A. S. KOBAYASHI and H. S. YOON, *ibid.* **73** (1990) 1382.
12. K. T. FABER and A. G. EVANS, *Acta Metall.* **31** (1983) 565.
13. *Idem, ibid.* **31** (1983) 577.
14. G. PEZZOTTI, *Acta Metall. Mater.* **41** (1993) 1825.
15. A. KELLY, "Strong solids" (Clarendon Press, Oxford, 1966) p. 131.
16. J. SELSING, *J. Amer. Ceram. Soc.* **44** (1961) 419.
17. J. HOMENY, W. L. VAUGHN and M. K. FERBER, *ibid.* **73** (1990) 394.
18. Y. K. BAEK and C. H. KIM, *J. Mater. Sci.* **24** (1989) 1589.
19. D. B. MARSHALL, *J. Amer. Ceram. Soc.* **67** (1984) C259.
20. D. B. MARSHALL and W. C. OLIVER, *ibid.* **70** (1987) 542.
21. U. V. DESHMUKH and T. W. COYLE, *Ceram. Engng. Sci. Proc.* **9** (1988) 627.
22. T. P. WEIHS and W. D. NIX, *J. Amer. Ceram. Soc.* **74** (1991) 524.
23. R. J. KERANS and T. A. PARTHASARATHY, *ibid.* **74** (1991) 1585.
24. D. B. MARSHALL, *Acta Metall. Mater.* **40** (1992) 427.
25. A. G. EVANS and R. M. McMEEKING, *Acta Metall.* **34** (1986) 2435.
26. P. F. BECHER, C.-H. HSUEH, P. ANGELINI and T. N. TIEGS, *J. Amer. Ceram. Soc.* **71** (1988) 1050.
27. G. H. CAMPBELL, M. RÜHLE, B. J. DALGLEISH and A. G. EVANS, *ibid.* **73** (1990) 521.
28. S. V. NAIR, *ibid.* **73** (1990) 2839.
29. P. F. BECHER, E. R. FULLER JR and P. ANGELINI, *ibid.* **74** (1991) 2131.
30. M. RÜHLE, B. J. DALGLEISH and A. G. EVANS, *Scripta Metall.* **21** (1987) 681.
31. J. RÖDEL, E. R. FULLER and B. R. LAWN, *J. Amer. Ceram. Soc.* **74** (1991) 3154.
32. F. F. LANGE, *Phil. Mag.* **22** (1970) 983.
33. R. M. McMEEKING and A. G. EVANS, *J. Amer. Ceram. Soc.* **65** (1982) 242.
34. B. BUDIANSKY, J. W. HUTCHINSON and J. C. LAMBROPOULOS, *Int. J. Solids Struct.* **19** (1983) 337.
35. D. B. MARSHALL, M. C. SHAW, R. H. DAUSKARDT, R. O. RITCHIE, M. J. READEY and A. H. HEUER, *J. Amer. Ceram. Soc.* **73** (1990) 2659.
36. I.-W. CHEN, *ibid.* **74** (1991) 2564.
37. A. G. EVANS and R. M. CANNON, *Acta Metall.* **34** (1986) 761.
38. N. CLAUSSEN, *Mater. Sci. Engng.* **71** (1985) 23.
39. D. B. MARSHALL and J. E. RITTER, *Amer. Ceram. Soc. Bull.* **66** (1987) 309.
40. A. G. EVANS and A. H. HEUER, *J. Amer. Ceram. Soc.* **63** (1980) 241.
41. N. CLAUSSEN, "Advances in ceramics", Vol. 12, edited by N. Claussen, M. Rühle and A. H. Heuer (American Ceramic Society, Columbus, OH, 1984) p. 325.
42. R. H. J. HANNINK, *Mater. Forum* **11** (1988) 43.
43. J. WANG and R. STEVENS, *J. Mater. Sci.* **24** (1989) 3421.
44. A. G. EVANS, "Advances in ceramics", Vol. 12, edited by N. Claussen, M. Rühle and A. H. Heuer (American Ceramic Society, Columbus, OH, 1984) p. 193.
45. M. RÜHLE, *Mater. Sci. Engng.* **105–6A** (1988) 77.
46. A. KRELL, P. BLANK and T. WEISS, *J. Mater. Sci.* **22** (1987) 3304.
47. K. R. WILFINGER and W. R. CANNON, *J. Amer. Ceram. Soc.* **72** (1989) 1256.
48. I. M. LOW, *J. Mater. Sci. Lett.* **7** (1988) 297.
49. A. E. GIANNAKOPOULOS and K. BREDER, *J. Amer. Ceram. Soc.* **74** (1991) 194.
50. M. BENGISU, O. T. INAL and O. TOSYALI, *Acta Metall. Mater.* **39** (1991) 2509.
51. J. HOMENY, W. L. VAUGHN and M. K. FERBER, *Amer. Ceram. Soc. Bull.* **66** (1987) 333.
52. J. LIU and P. D. OWNBY, *J. Amer. Ceram. Soc.* **74** (1991) 674.
53. K. TAKATORI, *J. Mater. Sci.* **26** (1991) 4484.
54. P. F. BECHER and G. C. WEI, *J. Amer. Ceram. Soc.* **67** (1984) 339.
55. G. C. WEI and P. F. BECHER, *Amer. Ceram. Soc. Bull.* **64** (1985) 298.
56. T. N. TIEGS and P. F. BECHER, *ibid.* **66** (1987) 339.
57. J. R. PORTER, F. F. LANGE and A. H. CHOKSHI, *ibid.* **66** (1987) 343.
58. S. LIO, M. WATANABE, M. MATSUBARA and Y. MATSUO, *J. Amer. Ceram. Soc.* **72** (1989) 1880.
59. S. M. SMITH, J. P. SINGH and R. O. SCATTERGOOD, *ibid.* **76** (1993) 497.
60. K. NIIHARA, A. NAKAHIRA, T. UCHIYAMA and T. HIRAI, "Fracture mechanics of ceramics", Vol. 7, edited by

R. C. Bradt, A. G. Evans, D. P. H. Hasselman and F. F. Lange (Plenum Press, New York, NY, 1986) p. 103.
61. Y.-S. CHOU and D. J. GREEN, *J. Amer. Ceram. Soc.* **76** (1993) 1452.
62. J. LIU and P. D. OWNBY, *ibid.* **74** (1991) 241.
63. N. CLAUSSEN, J. STEEB and R. F. PABST, *Amer. Ceram. Soc. Bull.* **56** (1977) 559.
64. D.-W. SHIN, K. K. ORR and H. SCHUBERT, *J. Amer. Ceram. Soc.* **73** (1990) 1181.
65. H. YOSHIMATSU, Y. MIURA, A. OSAKA, H. KAWASAKI and S. OHMORI, *J. Mater. Sci.* **25** (1990) 5231.
66. Q. L. GE, T. C. LEI and Y. ZHOU, *Mater. Sci. Technol.* **7** (1991) 490.
67. B. L. KARIHALOO, *J. Amer. Ceram. Soc.* **74** (1991) 1703.
68. J. WANG and R. STEVENS, *J. Mater. Sci.* **23** (1988) 804.
69. S. C. SAMANTA and S. MUSIKANT, *Ceram. Engng. Sci. Proc.* **6** (1985) 663.
70. R. RUH, K. S. MAZDIYASNI and M. G. MENDIRATTA, *J. Amer. Ceram. Soc.* **71** (1988) 503.
71. M. I. OSENDI, B. A. BENDER and D. LEWIS, *ibid.* **72** (1989) 1049.
72. J. S. MOYA and M. I. OSENDI, *J. Mater. Sci.* **19** (1984) 2909.
73. P. F. BECHER and T. N. TIEGS, *J. Amer. Ceram. Soc.* **70** (1987) 651.
74. M. G. CAIN and M. H. LEWIS, *ibid.* **76** (1993) 1401.
75. W. RAFANIELLO, K. CHO and A. V. VIRKAR, *J. Mater. Sci.* **16** (1981) 3479.
76. C. H. McMURTRY, W. D. G. BOECKER, S. G. SESHADRI, J. S. ZANGHI and J. E. GARNIER, *Amer. Ceram. Soc. Bull.* **66** (1987) 325.
77. H. ENDO, M. UEKI and H. KUBO, *J. Mater. Sci.* **26** (1991) 3769.
78. S. T. BULJAN, J. G. BALDONI and M. L. HUCKABEE, *Amer. Ceram. Soc. Bull.* **66** (1987) 347.
79. G. PEZZOTTI, I. TANAKA, T. OKAMOTO, M. KOIZUMI and Y. MIYAMOTO, *J. Amer. Ceram. Soc.* **72** (1989) 1461.
80. H. KODAMA, T. SUZUKI, H. SAKAMOTO and T. MIYOSHI, *ibid.* **73** (1990) 678.
81. Y. GOTO and A. TSUGE, *ibid.* **76** (1993) 1420.
82. J. HOMENY and L. J. NEERGAARD, *ibid.* **73** (1990) 3493.
83. T.-I. MAH and M. G. MENDIRATTA, *Amer. Ceram. Soc. Bull.* **60** (1981) 1229.
84. S. LIO, H. YOKOI, M. WATANABE and Y. MATSUO, *J. Amer. Ceram. Soc.* **74** (1991) 296.
85. A. KAMIYA, K. NAKANO and A. KONDOH, *J. Mater. Sci. Lett.* **8** (1989) 566.
86. R. TELLE and G. PETZOW, *Mater. Sci. Engng.* **105–6A** (1988) 97.
87. D. H. CHUNG and G. SIMMONS, *J. Appl. Phys.* **39** (1968) 5316.
88. P. F. BECHER, T. N. TIEGS, J. C. OGLE and W. H. WARWICK, "Fracture mechanics of ceramics", Vol. 7, edited by R. C. Bradt, A. G. Evans, D. P. H. Hasselman and F. F. Lange (Plenum Press, New York, NY, 1986) p. 61.
89. K. XIA and T. G. LANGDON, "Advanced composites '93", edited by T. Chandra and A. K. Dhingra (The Minerals, Metals and Materials Society, Warrendale, PA, 1993) p. 1181.
90. M. C. SHAW and K. T. FABER, "Ceramic microstructures '86: Role of interfaces", edited by J. A. Pask and A. G. Evans (Plenum Press, New York, NY, 1987) p. 929.
91. T. N. TIEGS and P. F. BECHER, *J. Amer. Ceram. Soc.* **70** (1987) C109.
92. M. G. JENKINS, A. S. KOBAYASHI, K. W. WHITE and R. C. BRADT, *ibid.* **70** (1987) 393.
93. M. RÜHLE, N. CLAUSSEN and A. H. HEUER, *ibid.* **69** (1986) 195.
94. M. RÜHLE, A. G. EVANS, R. M. McMEEKING and P. G. CHARALAMBIDES, *Acta Metall.* **35** (1987) 2701.
95. P. F. BECHER, *J. Amer. Ceram. Soc.* **66** (1983) 485.
96. A. C. SOLOMAH, W. REICHERT, V. RONDINELLA, L. ESPOSITO and E. TOSCANO, *ibid.* **73** (1990) 740.
97. P. D. SHALEK, J. J. PETROVIC, G. F. HURLEY and F. D. GAC, *Amer. Ceram. Soc. Bull.* **65** (1986) 351.
98. R. LUNDBERG, L. KAHLMAN, R. POMPE and R. CARLSSON, *ibid.* **66** (1987) 330.

Received 1 February 1994
and accepted 29 March 1994